

periodicity and very sharp rise times.

Alternatively, impulsive acceleration of electrons and protons in the magnetotail of the planet is an attractive possibility since it can account for the major features of the B and C events. There are several analogies which can be made with the phenomena observed in the earth's magnetotail, such as the so-called substorm effect in which electrons and protons are accelerated as a result of a sudden instability occurring in the magnetic tail region.

The phenomena we discovered at Mercury, however, place more stringent conditions on allowed models for impulsive acceleration than have heretofore been possible in studies of the earth's magnetosphere. For example, the rise times for each proton burst—and therefore the time limit for energizing protons to ≈ 0.5 Mev—is less than the time required for a proton to undergo one cyclotron period in the magnetic field (which we have assumed to be $\sim 5 \times 10^{-4}$ gauss). Therefore, no theories or models for magnetic field interactions involving many cyclotron periods can be operative. The consequence of this conclusion is that models invoking strong, impulsive electric fields appear to be required for the simultaneous acceleration of protons and electrons. For example, ion-acoustic wave acceleration (12) and even slow neutral sheet merging of magnetic fields may not account for the observations. The question of whether phenomena such as fast neutral sheet merging, sheet pinch instabilities (13), or runaway processes (14) can account for the postulated impulsive acceleration remains to be explored later.

The periodic oscillation of the electron intensity in the B and C events without accompanying periodic variations in the local magnetic field points strongly to the acceleration region as the source of the oscillation or "ringing effect." Indeed, this is fully supported by the series of impulsive proton bursts accompanying electron oscillations in the C event (Fig. 4). This effect will undoubtedly place strong constraints on models to be developed for explaining the impulsive acceleration of the particles.

Mercury's magnetosphere can provide sufficient energy for the observed bursts of electron and proton fluxes. We find that the maximum rate of energy input required to accelerate the protons and electrons we observed in the B event is $< 10^{-2}$ of the rate of energy input of the solar wind into the

magnetosphere. Therefore the mechanism of acceleration must also be very efficient. Since the energy spectra of the protons and electrons undoubtedly extend to lower energies and higher flux levels below our observational thresholds, it is quite clear that although there is sufficient energy via the solar wind-magnetic field-charged particle interactions, the energy spectra of protons and electrons must turn over below the detection thresholds in our experiment in order not to exceed the magnetic field energy density.

Clearly, a second encounter of Mariner 10 with Mercury through the magnetotail region of the planet would be of major importance for resolving the remaining questions on impulsive acceleration of Mercury's electron and proton fluxes.

J. A. SIMPSON, J. H. ERAKER
J. E. LAMPOR, P. H. WALPOLE
Enrico Fermi Institute, University of Chicago, Chicago, Illinois 60637

References and Notes

1. S. J. Bame, H. S. Bridge, L. A. Frank, J. W. Freeman, K. W. Ogilvie, C. W. Snyder, J. H. Wolfe, C. M. Yeates, "Final report of the plasma instrument team for the 1973 Mercury/Venus mission design study," preprint.
2. J. A. Simpson, S. M. Krimigis, J. E. Lamport, C. O. Bostrom, J. W. Kohl, W. T. Huntress, Jr., *JPL Document 615-5* (Jet Propulsion Laboratory, Pasadena, Calif., 1970).
3. P. Goldreich and S. J. Peale, *Astron. J.* **71**, 425 (1966).
4. N. F. Ness and Y. C. Whang, *J. Geophys. Res.* **76**, 1316 (1971).
5. F. C. Michel, *Comments Astrophys. Space Sci.* **3**, 27 (1971).
6. N. F. Ness, K. W. Behannon, R. P. Lepping, Y. C. Whang, K. H. Schatten, *Science* **185**, 151 (1974).
7. K. W. Ogilvie *et al.*, *ibid.*, p. 145.
8. J. A. Dunne, *ibid.* **183**, 1289 (1974); *ibid.* **185**, 141 (1974).
9. J. A. Simpson, J. H. Eraker, J. E. Lamport, P. H. Walpole, *ibid.* **183**, 1318 (1974).
10. J. A. Simpson, D. C. Hamilton, R. B. McKibben, A. Mogro-Campero, K. R. Pyle, A. J. Tuzzolino, *J. Geophys. Res.*, in press.
11. R. B. Blackman and J. W. Tukey, *The Measurement of Power Spectra* (Dover, New York, 1958).
12. F. L. Scarf, W. Bernstein, R. W. Fredricks, *J. Geophys. Res.* **70**, 9 (1965); R. W. Fredricks, F. L. Scarf, W. Bernstein, *ibid.*, p. 21.
13. B. Coppi, G. Laval, R. Pellet, *Phys. Rev. Lett.* **16**, 1207 (1966).
14. M. J. Houghton, preprint.
15. We wish to acknowledge the support of many individuals and groups which made these experiments possible. At the University of Chicago the instrument was designed and built in the Laboratory for Astrophysics and Space Research of the Enrico Fermi Institute and the preparation of programs and preliminary analysis were undertaken by G. Lentz, J. Coates, S. Christon, S. Daly, and A. J. Tuzzolino. The laboratory electron calibrations were carried out with the assistance of R. Zamow. We thank E. N. Parker for a valuable discussion of our results. At the Jet Propulsion Laboratory we are especially grateful for the support of W. Giberson, J. Dunne, A. Matzke, D. Swenson, and J. Tupman. It is clear that this mission could not have been successful without the strong support of J. E. Naugle, N. W. Cunningham, and S. E. Dwornik at NASA Headquarters. This research was supported in part by JPL contract 953091, NASA grant NGL 14-001-006, and NSF grant GA-38913X.

14 June 1974

Mercury's Atmosphere from Mariner 10: Preliminary Results

Abstract. *Analysis of data obtained by the ultraviolet experiment on Mariner 10 indicates that Mercury is surrounded by a thin atmosphere consisting in part of helium. The partial pressure of helium at the terminator is about 5×10^{-12} millibar. The total surface pressure of the atmosphere is less than about 2×10^{-9} millibar. Upper limits are set for the abundance of various gases, including hydrogen, oxygen, carbon, argon, neon, and xenon. The wavelength dependence of Mercury's surface albedo is similar to that of the moon over a broad range of wavelengths from 500 to 1600 angstroms. Strong signals were recorded by the airglow instrument as Mariner 10 passed through the cavity behind Mercury. They are as yet unexplained but may provide information on the properties of the local plasma.*

Two instruments sensitive in the extreme ultraviolet were carried aboard Mariner 10: an occultation spectrometer to measure the extinction properties of the atmosphere as the sun is occulted by the limbs of the planet, and a spectrometer to search for airglow at wavelengths selected to identify specific atmospheric gases. The airglow instrument has previously observed constituents in the upper atmospheres of the earth and Venus (1).

We concentrated attention on noble gases such as He, Ar, and Ne, since

there are several obvious supply processes for these gases. Helium and neon can be captured from the solar wind; helium and argon may be released by decay of radioactive elements in Mercury's crustal rocks. A preliminary examination of the mass balance for the various species on Mercury leads us to conclude that the most probable species would be Ar, Ne, and He. The choice of airglow channels reflects this analysis. However, the instrument was also designed to detect emissions associated with H, O, and C.

Occultation experiment. The absorption cross sections of all common atmospheric gases and their photochemical products are large in the extreme ultraviolet (300 to 900 Å). Values for absorption cross sections range from 1×10^{-17} to 7×10^{-17} cm². Since the sun is a bright source of extreme ultraviolet radiation, the occultation experiment provides a sensitive test for the presence of an atmosphere almost regardless of its composition.

The occultation spectrometer has a plane grating which operates at grazing incidence (2). Channel electron multipliers measure the solar flux at four wavelength positions, 470, 740, 810, and 890 Å, chosen to straddle the first ionization edges of Ne, He, Ar, and Kr. Pinholes isolate spectral bands of ~ 75 Å full width at half maximum (FWHM) and also define the effective field of view of the instrument, which is 0.15° FWHM. The instrument, which is body-fixed to the spacecraft, observed the sun continuously for several days during Mercury encounter. The solar flux was sampled in each channel every 0.6 second. Raw data received at ingress and egress are plotted in Fig. 1.

There are no obvious effects in these data due to atmospheric extinction. The intensity variations that are evident are due to the motion of the projected field of view of the instrument on the solar disk. This motion is caused by the spacecraft's limit cycle motion (3). The characteristic time scale for atmospheric effects is quite short (1 to 50 seconds) and is determined by the velocity of the spacecraft (approximately 11 km/sec) as it passes behind Mercury, the scale height (H) in the planet's atmosphere, and the angular field of view of the instrument. At encounter the height resolution at the occulting limb was about 16 km. In the absence of an atmosphere the signal cutoff should occur in about 2.4 data sample periods. The observed cutoff took place, in all channels, within three data samples,

Fig. 2. (a) Geometry of the field of view with respect to the planet at encounter minus 1 hour. The field of view is 0.13° by 3.6° . The planet was at a range of 43,000 km. A 5° slew was used at a rate of $\frac{1}{8}$ sec⁻¹. The data taken during this scan are shown in Fig. 3. (b) Geometry of the field of view with respect to the planet during the limb drift experiment 21 minutes before closest approach. The planetary phase angle is 114° and the range to the limb is $\sim 12,400$ km.

Table 1. Upper limits to the abundances of atmospheric constituents on Mercury deduced from the ultraviolet observations. The data were obtained on 29 March 1974 at 2028 G.M.T. The 0.13° field of view was 15 km above the bright limb at a range of 12,400 km. A temperature of 550°K was assumed in calculating the vertical column densities. These data are not corrected for background.

Probable emitting species	Channel (Å)	Upper limit to limb brightness (rayleighs)	g-Value at Mercury (photon sec ⁻¹ atom ⁻¹)	Vertical column density (cm ⁻²)	Partial pressure (mbar)
He ⁺	304	1200			
Background	430				
He	584	84	2.0×10^{-5}	7×10^{11}	2×10^{-12}
Ne	740	23	5.1×10^{-5}	3×10^{13}	4×10^{-10}
Ar	869	85	4.2×10^{-7}	1×10^{13}	3×10^{-10}
Ar	1048	150	1.4×10^{-6}	5×10^{12}	
H	1216	5000	1.5×10^{-2}	1×10^{11}	1×10^{-13}
O	1304	240	1.3×10^{-1}	1×10^{11}	2×10^{-12}
Xe (1470 Å)	1480	490	1.0×10^{-5}	1×10^{12}	1×10^{-10}
C	1657	870	1.4×10^{-3}	5×10^{10}	4×10^{-13}

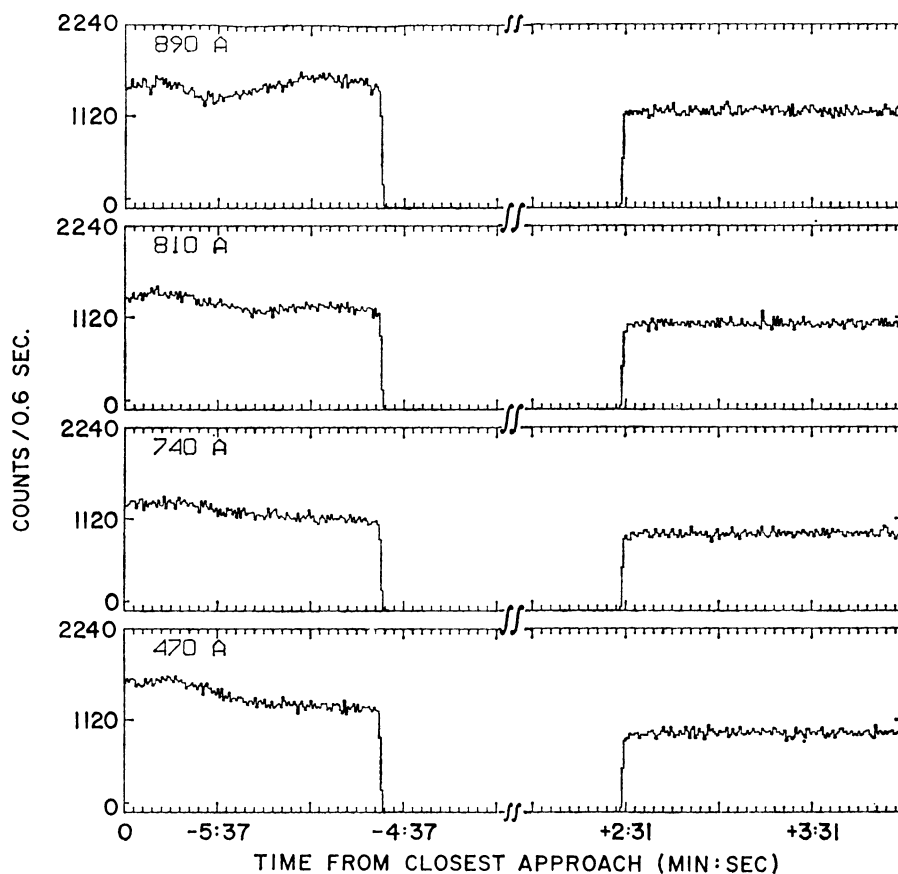


Fig. 1. Sample of data from the occultation spectrometer as the spacecraft moved into and out of occultation at Mercury.

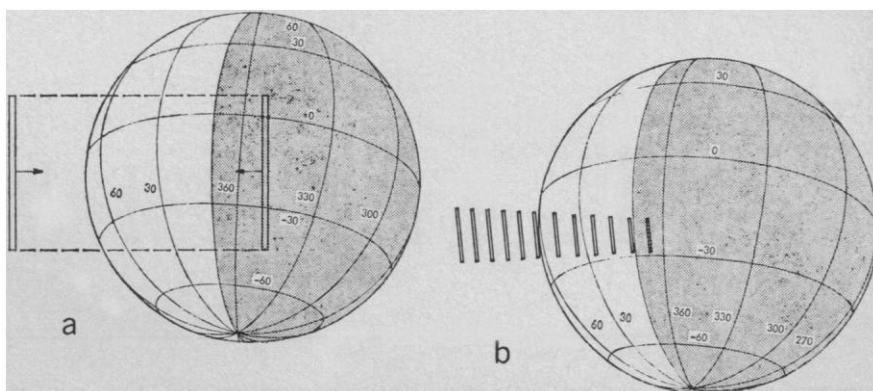
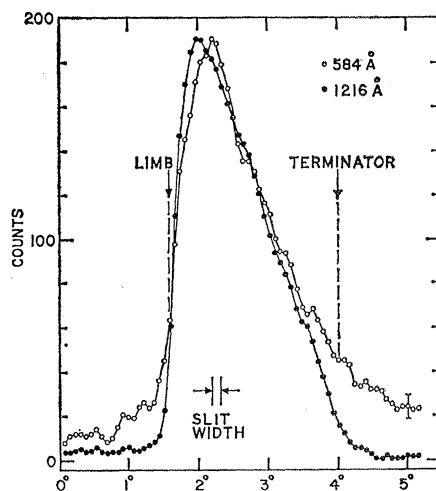


Fig. 3. Data obtained from the sequence shown in Fig. 2a. Counts from the four scans were summed and smoothed. The 1216-Å data were scaled by a factor of 0.63 for comparison. Points on the 584-Å curve represent the number of counts accumulated in 2.4 seconds.



consistent with a sharp edge—that is, planetary limb occultation.

An estimate of the maximum possible attenuation, 16 km above the limb, gives an upper limit to any atmosphere on Mercury. We feel that a drop in intensity in the last few samples of more than 10 percent is excluded by the data. This corresponds to a maximum vertical optical depth of $8 \times 10^{-4} H^{1/2}$ in the extreme ultraviolet. Here H is measured in kilometers. For CO_2 near the terminator, at an assumed temperature of 100°K , this corresponds to an upper limit of $4 \times 10^{13} \text{ cm}^{-2}$ for the column density or a surface pressure of 1×10^{-9} mbar. This decreases the best previous limit on the surface pressure for CO_2 [approximately 2×10^{-5} mbar (4)] by a factor of 2×10^4 . For He and Ar the limits for the column densities are 4×10^{14} and $8 \times 10^{13} \text{ cm}^{-2}$, respectively; the corresponding surface pressures are 1×10^{-9} and 2×10^{-9} mbar.

Considerable improvement in these figures is anticipated with further processing of the data. Signal variations due to the limit cycle motion of the field of view on the sun can be removed in the following way: Data from the many hours of observation preceding and following the encounter

can be used to build up an intensity picture of the sun as a function of the spacecraft attitude sensor signals, and a correction can then be applied to the data taken at occultation.

Airglow experiment. The airglow spectrometer (1) has ten detectors which accept emission over 20-Å bandwidths about the central wavelengths 304, 430, 584, 740, 869, 1048, 1216, 1304, 1480, and 1657 Å. These wavelengths correspond to the positions of strong lines of He^+ , He, Ne, Ar, H, O, and C (see Table 1). In addition, there are two zero-order channels which provide checks on the total incident extreme ultraviolet flux to the spectrometer. One of these channels is open, the other has a MgF_2 filter and CuI photocathode. The instrument is mounted on the scan platform which provides considerable pointing versatility. The effec-

tive field of view of the instrument is 0.13° by 3.6° .

The sequence of operation at Mercury consisted of three separately identifiable modes: (i) A mode in which the instrument was moved at a constant rate, $1/8^\circ$ per second, by the spacecraft scan platform, as illustrated in Fig. 2a. At 1, 2, and 4 hours before encounter, four scans were made across the planet. (ii) A fixed pointing mode in which the objective was to build up the signal to a statistically significant total count in each channel. (iii) A drift mode in which the field of view moves across the limb as a result of spacecraft motion. This is illustrated in Fig. 2b. Limb drifts were performed 21 minutes before encounter and 9 minutes after encounter. The latter gave the highest spatial resolution (~ 15 km) at the limb.

Figure 3 shows the results of four scans made across the planet at 1 hour before encounter. Only the data from the 1216- and 584-Å channels are shown. Individual scans have been summed and smoothed. A significant signal is seen in the 584-Å channel. The signal extends beyond the bright limb and well into the dark side across the terminator. The signal in the 1216-Å channel rises abruptly at the limb and falls to the background level at the geometrical terminator; it is similar to the signal in the zero-order channels, which is predominantly due to sunlight scattered from the surface of the planet.

We interpret these data for the 584-Å channel as indicating the definite presence of neutral He on the planet. Further processing of the data is required to remove the effects of limit cycle motion before the actual distribution of intensity can be derived. However, a preliminary estimate of the brightness at the terminator is about 45 rayleighs. The derivation of global He abundance requires proper modeling. The effects of scattering of sunlight, of collisional processes, surface albedo, solar wind interaction, and variable surface temperature should be included. However, if the 584-Å emission is entirely due to single scattering in a homogeneous atmosphere, then the vertical column density of neutral He atoms near the terminator would be $2 \times 10^{12} \text{ cm}^{-2}$, well below the exospheric limit of $\sim 10^{15} \text{ cm}^{-2}$ (5). The observed column density corresponds to a He partial pressure of 5×10^{-12} mbar near the terminator.

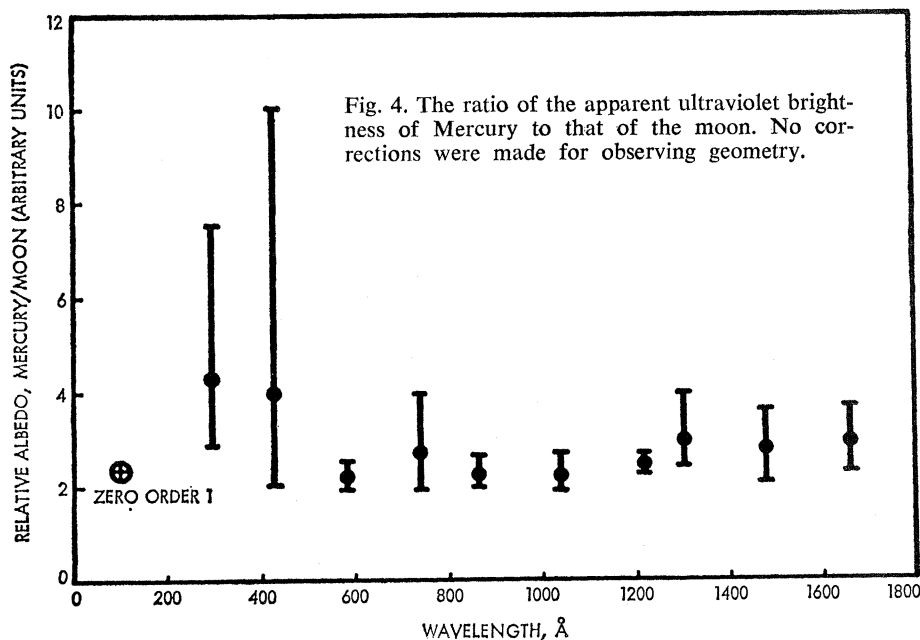


Fig. 4. The ratio of the apparent ultraviolet brightness of Mercury to that of the moon. No corrections were made for observing geometry.

If He is lost primarily by thermal escape, we estimate that the atmospheric residence time should be of the order of 10^5 seconds. The source strength required to supply the observed He atmosphere would then be of the order of $10^7 \text{ cm}^{-2} \text{ sec}^{-1}$, which is comparable to the He source in the earth's atmosphere (6).

The drift sequence across the bright limb (Fig. 2b) provides stringent upper limits to the abundances of probable atmospheric constituents. These are listed in Table 1 and were estimated from data taken 15 km above the limb. For these calculations we have assumed the local surface temperature at the limb to be 550°K (7). Scattering efficiencies and g -values for the resonance emissions of H, O, C, and Xe were scaled from the compilations of Barth (8) and Fastie *et al.* (9). For the other species the g -values were based on reported solar fluxes (10), oscillator strengths (11), and assumed solar line widths (12).

Inspection of the results in Table 1 shows that the airglow spectrometer is far more sensitive to individual species than the occultation instrument. Of particular interest is Ar, which should be produced radiogenically in the planet. If we assume that Ar is removed primarily by interaction with the solar wind, we can deduce an upper limit to the supply rate. Its residence time should be similar to the ionization time of the gas, that is, $\sim 10^6$ seconds. Combining this number with the column density upper limit in Table 1, we find a maximum source strength of $\sim 10^7 \text{ cm}^{-2} \text{ sec}^{-1}$. This is consistent with the terrestrial supply rate of $2 \times 10^5 \text{ cm}^{-2} \text{ sec}^{-1}$ (6).

During the Mercury encounter channels at wavelengths short of 1216 \AA observed sporadic emission. This emission was seen during the limb drifts and while observations were being made of the dark side of the planet. The spacecraft was also within the solar wind cavity during most of these bursts of emission, but we have found little correlation with the fluxes observed by the plasma and energetic particle experiments (13).

Extreme ultraviolet albedo. Observations of the bright side of the moon were obtained with the airglow instrument shortly after launch. These were compared with similar measurements on Mercury made several hours before encounter. The ratio of the apparent brightnesses is plotted in Fig. 4 on an

arbitrary scale. The marked similarity between the two is obvious in spite of the poor statistics in the two short-wavelength channels at 304 and 430 \AA . Evidently the similarity of the run of albedo with wavelength between Mercury and the moon that has been reported throughout the visible (14) extends far into the ultraviolet and probably at least down to wavelengths of 500 \AA .

Conclusions. The Mariner 10 ultraviolet spectrometer experiment has achieved its primary objective of detecting a neutral atmosphere on Mercury. Evidently neutral He is a prime constituent. The column density is very low, such that the atmospheric atoms follow ballistic trajectories. The occultation experiment places an exceedingly low limit to the total atmospheric content, far lower than indicated by any previous measurements. Further reductions in these limits are expected when the effects of spacecraft limit cycle motion are included in the analysis. Similarly, further analysis should provide information on the neutral He scale height and also on the origin of the unexpected "emission" seen as the spacecraft flew behind Mercury.

A. L. BROADFOOT
S. KUMAR
M. J. S. BELTON

*Kitt Peak National Observatory,
Tucson, Arizona 85726*

M. B. MCELROY
*Harvard University,
Cambridge, Massachusetts 02138*

References and Notes

1. A. L. Broadfoot, S. Kumar, M. J. S. Belton, M. B. McElroy, *Science* **183**, 1315 (1974).
2. J. A. R. Samson, *Techniques of Vacuum Ultraviolet Spectroscopy* (Wiley, New York, 1967), p. 76.
3. The solar disk had an angular diameter of 1.18° at Mercury encounter. The intensity distribution in the extreme ultraviolet is very inhomogeneous over the disk [see E. M. Reeves and W. H. Parkinson, *Astrophys. J. Suppl.* **21**, 1 (1970)]. The spacecraft limit cycle was $\pm 0.3^\circ$ in all three axes.
4. U. Fink, H. P. Larsen, R. F. Poppen, *Astrophys. J.* **187**, 407 (1974).
5. M. J. S. Belton, D. M. Hunten, M. B. McElroy, *ibid.* **150**, 1111 (1967).
6. P. M. Banks, H. E. Johnson, W. I. Axford, *Comments Astrophys. Space Phys.* **2**, 214 (1970).
7. S. C. Chase, E. D. Miner, D. Morrison, G. Münch, G. Neugebauer, M. Schroder, *Science* **185**, 142 (1974).
8. C. A. Barth, *Appl. Opt.* **8**, 1295 (1969).
9. W. G. Fastie, P. D. Feldman, R. C. Henry, H. W. Moos, C. A. Barth, G. E. Thomas, T. M. Donahue, *Science* **182**, 710 (1973).
10. H. E. Hinteregger, *Ann. Geophys.* **26**, 547 (1970).
11. W. L. Wiese, M. W. Smith, B. M. Glennon, *Ref. Data Ser. U.S. Natl. Bur. Stand.* **1**, 4 (1966).
12. For the He 584-Å line, we have used the solar line width measured by G. Cushman, L. Farwell, G. Goden, and W. A. Rense (in preparation).
13. We wish to thank J. A. Simpson and H. S. Bridge for providing us with their unpublished data.
14. T. B. McCord and J. B. Adams, *Science* **178**, 745 (1972); *Icarus* **17**, 585 (1972).
15. We would like to express our appreciation for the assistance of Frank E. Stuart and the Electronics Laboratory at Kitt Peak National Observatory in construction of the instrument. We are especially grateful for the exceptional effort put forth by Sam S. Clapp, senior engineer at Kitt Peak. Special thanks are due to Jet Propulsion Laboratory personnel, particularly Clayne M. Yeates and James A. Dunne for providing the science support. We also thank D. G. Rea for a critical review of the manuscript. This research was sponsored by the National Aeronautics and Space Administration. Kitt Peak National Observatory is operated by the Association of Universities for Research in Astronomy, Inc., under contract with the National Science Foundation.

3 June 1974

Mercury's Surface: Preliminary Description and Interpretation from Mariner 10 Pictures

Abstract. The surface morphology and optical properties of Mercury resemble those of the moon in remarkable detail and record a very similar sequence of events. Chemical and mineralogical similarity of the outer layers of Mercury and the moon is implied; Mercury is probably a differentiated planet with a large iron-rich core. Differentiation is inferred to have occurred very early. No evidence of atmospheric modification of landforms has been found. Large-scale scarps and ridges unlike lunar or martian features may reflect a unique period of planetary compression near the end of heavy bombardment by small planetesimals.

Mariner 10 acquired 2300 television pictures in the vicinity of Mercury in order to investigate the geologic history of the planet as manifested in the morphology and optical properties of the surface. A unique surface history could have been indicated by the planet's Earth-like density (5.5 g/cm^3)

and small size (4870 km) (1). Instead, an extraordinary similarity to the surface of the moon has been found; the implications of this lunar-like exterior and probable Earth-like interior provide insight into very early stages of planetary formation.

A brief description of the first images